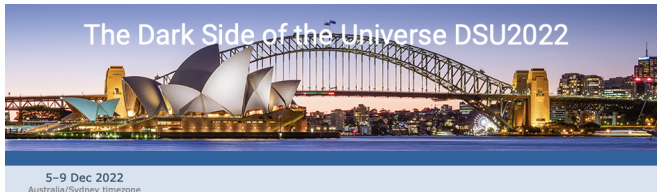


Thermal WIMPs and the Scale of New Physics

Ankit Beniwal

(On behalf of the GAMBIT Collaboration)

P. Athron et al., *Thermal WIMPs and the Scale of New Physics: Global Fits of Dirac Dark Matter Effective Field Theories*, EPJC 81 (2021) 11, 992, [arXiv:2106.02056]



Outline

- 1 Global fits and GAMBIT
- 2 Dirac fermion DM EFTs
- 3 Constraints and likelihoods
- 4 Results
- 5 Summary



Global fits and GAMBIT

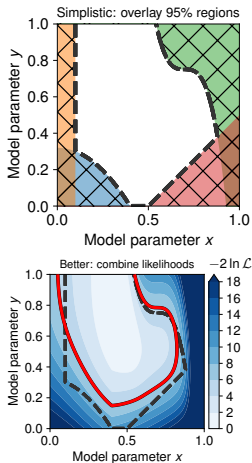
Theories with *many* free parameters/constraints?

- ① Construct a *composite likelihood* function:

$$\mathcal{L}_{\text{total}} = \mathcal{L}_{\text{DD}} \times \mathcal{L}_{\text{ID}} \times \mathcal{L}_{\text{Collider}} \times \dots$$

- ② Traditional sampling methods (random, grid) are inefficient.
S. S. AbdusSalam et al., [arXiv:2012.09874]
- ③ Explore parameter space using *advanced* sampling techniques (e.g., MCMC, nested sampling).
- ④ Interpret results in *frequentist* and/or *Bayesian* statistical frameworks.

→ GAMBIT



GAMBIT: The Global And Modular BSM Inference Tool

gambit.hepforge.org

github.com/GambitBSM

EPJC 77 (2017) 784

arXiv:1705.07908

- Extensive model database, beyond SUSY
- Fast definition of new datasets, theories
- Extensive observable/data libraries
- Plug&play scanning/physics/likelihood packages
- Various statistical options (frequentist /Bayesian)
- Fast LHC likelihood calculator
- Massively parallel
- Fully open-source



Members of: ATLAS, Belle-II, CLIC, CMS, CTA, Fermi-LAT, DARWIN, IceCube, LHCb, SHiP, XENON

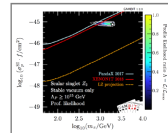
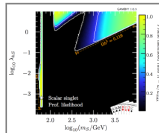
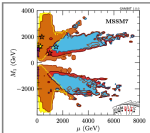
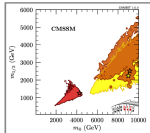
Authors of: BubbleProfiler, Capt'n General, Contur, DarkAges, DarkSUSY, DDCalc, DirectDM, Diver, EasyScanHEP, ExoCLASS, FlexibleSUSY, gamLike, GM2Calc, HEPLike, IsaTools, MARTY, nuLike, PhaseTracer, PolyChord, Rivet, SOFTSUSY, SuperIso, SUSY-AI, xsec, Vevacious, WIMPSim

Recent collaborators: P Athron, C Balázs, A Beniwal, S Bloor, T Bringmann, A Buckley, J-E Camargo-Molina, C Chang, M Chrzaszcz, J Conrad, J Cornell, M Danner, J Edsjö, T Emken, A Fowlie, T Gonzalo, W Handley, J Harz, S Hoof, F Kahlhoefer, A Kvellestad, P Jackson, D Jacob, C Lin, N Mahmoudi, G Martinez, MT Prim, A Raklev, C Rogan, R Ruiz, P Scott, N Serra, P Stöcker, W. Su, A Vincent, C Weniger, M White, Y Zhang, ++

70+ participants in many experiments and numerous major theory codes

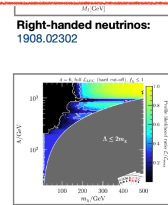
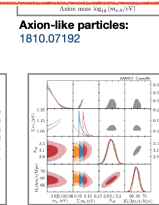
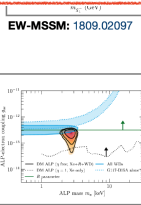
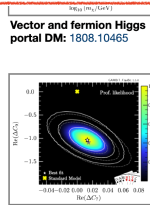


Recent GAMBIT studies



Chris Chang Tuesday @ 16:50 (Dark Matter) Global Fits of vector-mediated simplified models for Dark Matter

Csaba Balazs Friday @ 11:30 (Plenary) Dark Matter with GAMBIT



Flavour EFT: 2006.03489

More axion-like particles:
2006.03489

Neutrinos and cosmo:
2009.03287

Dark matter EFTs:
2106.02056

Slide courtesy:
A. Kvellestad, TOOLS 2021



- A Dirac fermion WIMP DM (χ) interacting with SM quarks or gluons via

$$\mathcal{L}_{\text{int}} = \sum_{a,d} \frac{\mathcal{C}_a^{(d)}}{\Lambda^{d-4}} \mathcal{Q}_a^{(d)}, \quad (1)$$

where $\mathcal{C}_a^{(d)}$ = dimensionless Wilson coefficients, Λ = scale of new physics, $d \leq 7$ and $\mathcal{Q}_a^{(d)}$ = DM-SM operators.

- Full Lagrangian is

$$\mathcal{L} = \mathcal{L}_{\text{SM}} + \mathcal{L}_{\text{int}} + \bar{\chi}(i\not{\partial} - \not{m}_{\chi})\chi. \quad (2)$$

- Free model parameters:

$$6 \ (d=6), \quad 16 \ (d=6 \ \& \ 7).$$

$$\begin{aligned}\mathcal{Q}_{1,q}^{(6)} &= (\bar{\chi}\gamma_\mu\chi)(\bar{q}\gamma^\mu q), \\ \mathcal{Q}_{2,q}^{(6)} &= (\bar{\chi}\gamma_\mu\gamma_5\chi)(\bar{q}\gamma^\mu q), \\ \mathcal{Q}_{3,q}^{(6)} &= (\bar{\chi}\gamma_\mu\chi)(\bar{q}\gamma^\mu\gamma_5 q), \\ \mathcal{Q}_{4,q}^{(6)} &= (\bar{\chi}\gamma_\mu\gamma_5\chi)(\bar{q}\gamma^\mu\gamma_5 q).\end{aligned}$$

Dimension-6 operators

$$\begin{aligned}\mathcal{Q}_1^{(7)} &= \frac{\alpha_s}{12\pi}(\bar{\chi}\chi)G^{a\mu\nu}G_{\mu\nu}^a, \\ \mathcal{Q}_2^{(7)} &= \frac{\alpha_s}{12\pi}(\bar{\chi}i\gamma_5\chi)G^{a\mu\nu}G_{\mu\nu}^a, \\ \mathcal{Q}_3^{(7)} &= \frac{\alpha_s}{8\pi}(\bar{\chi}\chi)G^{a\mu\nu}\tilde{G}_{\mu\nu}^a, \\ \mathcal{Q}_4^{(7)} &= \frac{\alpha_s}{8\pi}(\bar{\chi}i\gamma_5\chi)G^{a\mu\nu}\tilde{G}_{\mu\nu}^a, \\ \mathcal{Q}_{5,q}^{(7)} &= m_q(\bar{\chi}\chi)(\bar{q}q), \\ \mathcal{Q}_{6,q}^{(7)} &= m_q(\bar{\chi}i\gamma_5\chi)(\bar{q}q), \\ \mathcal{Q}_{7,q}^{(7)} &= m_q(\bar{\chi}\chi)(\bar{q}i\gamma_5 q), \\ \mathcal{Q}_{8,q}^{(7)} &= m_q(\bar{\chi}i\gamma_5\chi)(\bar{q}i\gamma_5 q), \\ \mathcal{Q}_{9,q}^{(7)} &= m_q(\bar{\chi}\sigma^{\mu\nu}\chi)(\bar{q}\sigma_{\mu\nu}q), \\ \mathcal{Q}_{10,q}^{(7)} &= m_q(\bar{\chi}i\sigma^{\mu\nu}\gamma_5\chi)(\bar{q}\sigma_{\mu\nu}q).\end{aligned}$$

Dimension-7 operators



Constraints and likelihoods

- **Mixing and threshold corrections:**

- For direct detection, $\mathcal{C}_a^{(d)}$'s required at energy scale $\mu = 2 \text{ GeV}$;
- Running/mixing of operators handled by DirectDM v2.2.0.

F. Bishara et al., [arXiv:1708.02678]; J. Brod et al., *JHEP*, [arXiv:1710.10218]

- Threshold corrections when μ is below/above a quark mass, e.g., m_t .

- **EFT validity:**

- ➊ $\Lambda \gtrsim 2 \text{ GeV}$ (direct detection);
- ➋ $\Lambda > 2m_\chi$ (relic density and indirect detection);
- ➌ $\not{E}_T < \Lambda$ (collider searches). Modify \not{E}_T spectrum when $\not{E}_T > \Lambda$:

$$\frac{d\sigma}{d\not{E}_T} \rightarrow \begin{cases} 0, & \text{hard cut-off,} \\ \frac{d\sigma}{d\not{E}_T} \left(\frac{\not{E}_T}{\Lambda} \right)^{-a}, & \text{smooth cut-off.} \end{cases} \quad (3)$$

Here $a \in [0, 4] = \text{nuisance parameter}$.

- **Perturbative couplings:** $|\mathcal{C}_a^{(d)}| < 4\pi$.

- **Parameter ranges:** $m_\chi \in [5, 500] \text{ GeV}$ and $\Lambda \in [20, 2000] \text{ GeV}$.



Constraints and likelihoods

❶ Direct detection (DirectDM v2.2.0 & DDCalc v2.2.0)

XENON1T; LUX (2016); PandaX (2016) and (2017); CDMSlite; CRESST-II and CRESST-III; PICO-60 (2017) and (2019); DarkSide-50

F. Bishara et al., [arXiv:1708.02678]; J. Brod et al., *JHEP*, [arXiv:1710.10218]; P. Athron et al., *EPJC*, [arXiv:1808.10465]

❷ Relic density (CalcHEP v3.6.27, GUM & DarkSUSY v6.2.2)

A. Belyaev et al., *CPC*, [arXiv:1207.6082]; S. Bloor et al., [arXiv:2107.00030]; T. Bringmann et al., *JCAP*, [arXiv:1802.03399]

❸ Fermi-LAT via gamma rays (gamLike v1.0.1)

T. Bringmann et al., *EPJC*, [arXiv:1705.07920]

❹ Solar capture (Capt'n General) and CMB bounds (CosmoBit)

N. Avis Kozar et al., arXiv:[2105.06810]; J. J. Renk et al., *JCAP*, [arXiv:2009.03286]

❺ ATLAS and CMS monojet searches (ColliderBit, FeynRules v2.0,

MadGraph_aMC@NLO v2.6.6, Pythia v8.1 & Delphes v3.4.2)

G. Aad et al., [arXiv:2102.10874]; A. M. Sirunyan et al., *PRD*, [arXiv:1712.02345]

C. Balazs et al., *EPJC*, [arXiv:1705.07919]; A. Alloul et al., *CPC*, [arXiv:1310.1921]

J. Alwall et al., *JHEP*, [arXiv:1106.0522]; T. Sjostrand et al., *CPC*, [arXiv:0710.3820]

J. de Favereau et al., *JHEP*, [arXiv:1307.6346]

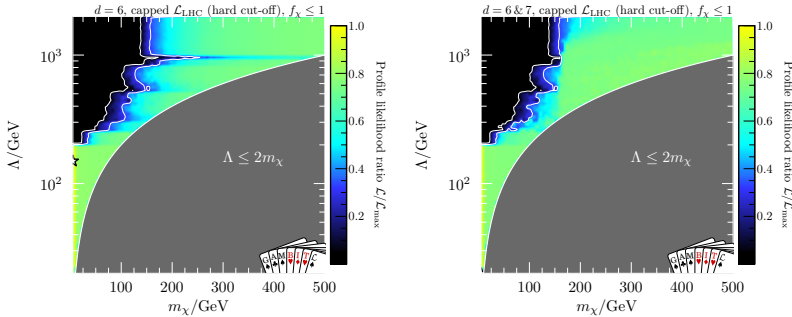
+ 8 nuisance parameters

Top-quark running mass, nuclear form factors, and astrophysical distribution of DM.



Results

Capped \mathcal{L}_{LHC} likelihood (hard cut-off), $f_\chi \equiv (\Omega_\chi + \Omega_{\bar{\chi}})/0.12 \leq 1$



Left panel: $d = 6$; **Right panel:** $d = 6 \& 7$; **White star** = best-fit point.

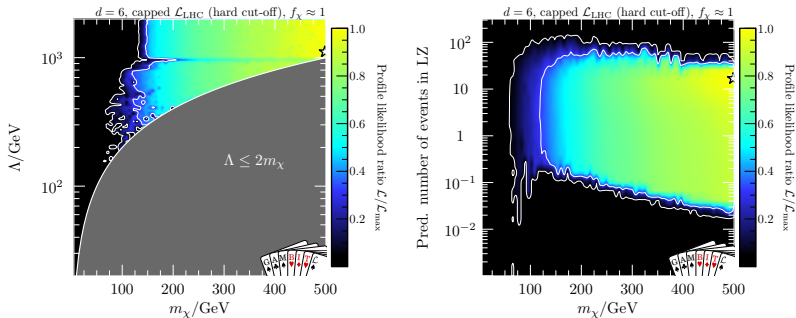
- Small m_χ and large Λ : strong constraints from LHC; impossible to satisfy relic density requirement. LHC constraints absent for $\Lambda < 200$ GeV.
- Slight upward fluctuation in *Fermi-LAT* data fitted by (for $d = 6$ case):

$$m_\chi = 5.0 \text{ GeV}, \quad f_\chi^2 \langle \sigma v \rangle_0 = 1.1 \times 10^{-27} \text{ cm}^3 \text{s}^{-1}. \quad (4)$$



Results

Capped \mathcal{L}_{LHC} likelihood (hard cut-off), $f_\chi \approx 1$

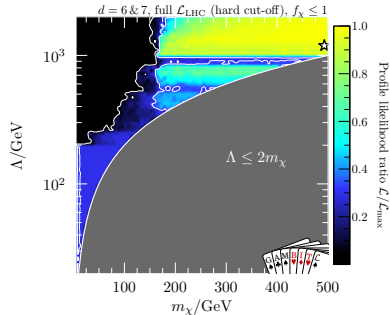
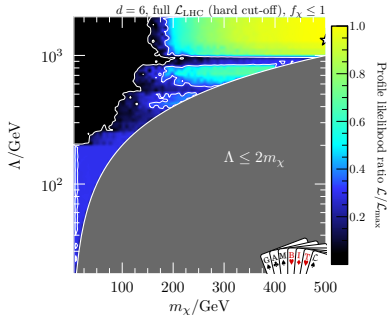


- Impossible to obtain $\Omega_\chi h^2 = 0.12$ for $m_\chi \lesssim 100 \text{ GeV}$; relic density requirement incompatible with *Fermi*-LAT and CMB bounds.
- Up to **10 events** predicted in LZ experiment \sim best-fit point \rightarrow require a non-zero $Q_2^{(6)}$ (spin-independent, momentum-suppressed interaction).



Results

Full \mathcal{L}_{LHC} likelihood (hard cut-off), $f_\chi \leq 1$



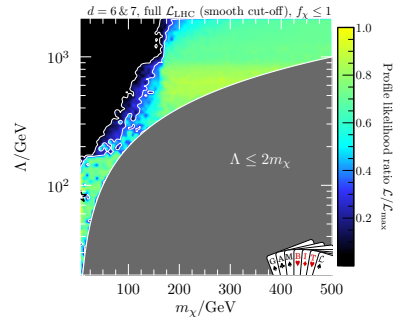
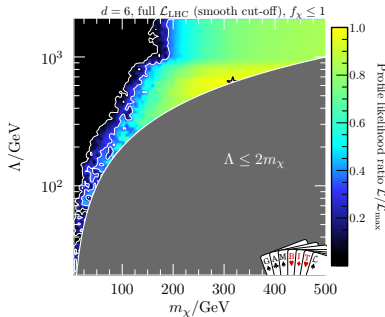
- For $d = 6$, excesses seen in few high- \cancel{E}_T bins in the ATLAS & CMS monojet searches. Preferred values for Λ at 1σ level:

$$\Lambda \approx 700 \text{ GeV} (\text{CMS}), \quad \Lambda \gtrsim 1 \text{ TeV} (\text{ATLAS}). \quad (5)$$

- Similar results for $d = 6 \& 7$ (right panel).

Results

Full \mathcal{L}_{LHC} likelihood (smooth cut-off), $f_\chi \leq 1$



- For $d = 6$, best-fit improves fit to both excesses (*Fermi-LAT* and LHC) simultaneously than in hard cut-off case (similar for $d = 6 \& 7$).
- Requires $\Lambda \sim 80 \text{ GeV}$ and soft cut-off $a \approx 1.7$ in the \cancel{E}_T spectrum.



- First global analysis of full set of effective operators ($d \leq 7$) for a Dirac fermion DM interaction with quarks/gluons.
- Novel approach addresses issue of EFT validity @ LHC via a cut-off parameter for $\cancel{E}_T > \Lambda$.
- Highly efficient likelihood calculations + sampling algorithms to sample 24 dimensions (m_χ , Λ , $14 \times C_a^{(d)}$ + 8 nuisance parameters).
- Strong constraints on small m_χ and large $\Lambda \rightarrow$ slight preference for DM signal at relatively small Λ .
- Large hierarchy *not possible* between m_χ and Λ without violating the relic density constraint.
- LHC constraints require $\Lambda \lesssim 200$ GeV for $m_\chi \lesssim 100$ GeV.
- Large viable regions of parameter space for $f_\chi \lesssim 1$.

All results, samples & input files publicly available via Zenodo:

<https://zenodo.org/record/4836397>

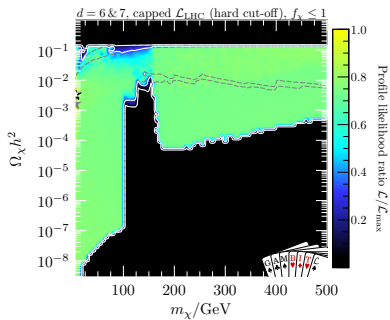
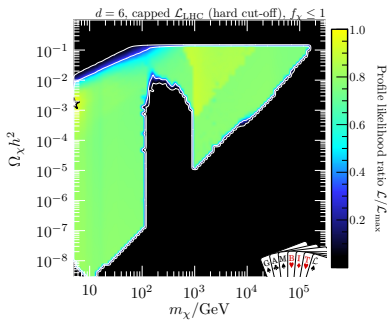


Backup slides



Supplementary results

Capped \mathcal{L}_{LHC} likelihood (hard cut-off), $f_\chi \leq 1$

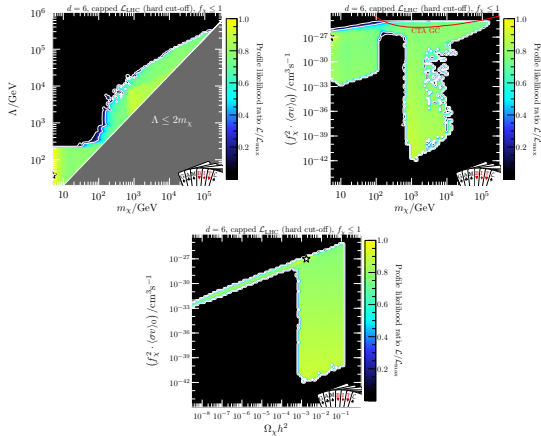


- For $d = 6$ and $m_\chi \lesssim 100 \text{ GeV}$, impossible to obtain $\Omega_\chi h^2 = 0.12$ with combined indirect and direct detection constraints.
- In $d = 6 \& 7$, now possible to saturate relic density bound for small m_χ (and small Λ) thanks to suppressed signals from $\mathcal{Q}_{3,q}^{(7)}$ and $\mathcal{Q}_{7,q}^{(7)}$.



Supplementary results

Capped \mathcal{L}_{LHC} likelihood (hard cut-off), $f_\chi \leq 1$



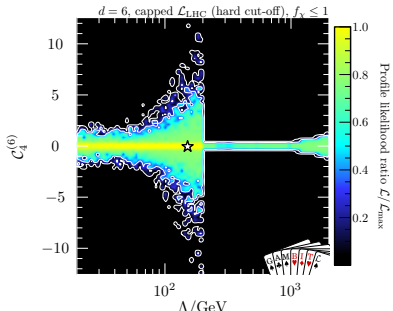
Left panel: (m_χ, Λ) plane. **Right panel:** $(m_\chi, f_\chi^2 \langle \sigma v \rangle_0)$ plane.

Bottom panel: $(\Omega_\chi h^2, f_\chi^2 \langle \sigma v \rangle_0)$ plane.

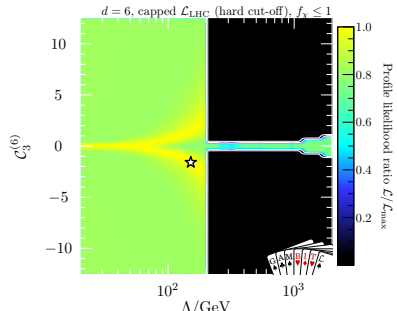


Supplementary results

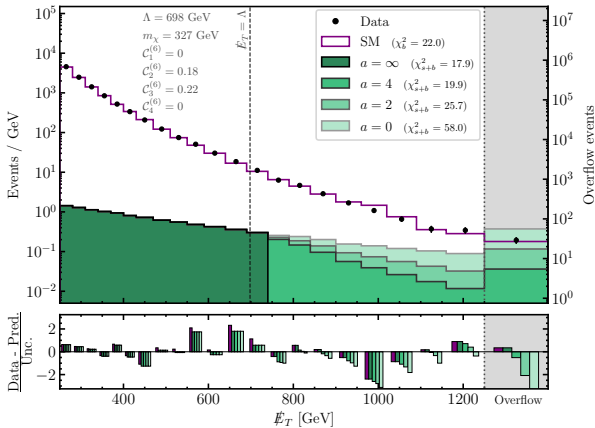
Capped \mathcal{L}_{LHC} likelihood (hard cut-off), $f_\chi \leq 1$



Left panel: $(m_\chi, C_4^{(6)})$ plane. Right panel: $(m_\chi, C_3^{(6)})$ plane.



Supplementary results



Top panel: Examples of missing transverse energy (\cancel{E}_T) spectrum for the CMS monojet search. **Bottom panel:** Pull ($\equiv (\text{data} - \text{predicted})/\text{uncertainty}$) per bin.



- ❶ **DarkBit** *EPJC*, [arXiv:1705.07920]
Relic density, indirect and direct detection.
- ❷ **SpecBit, DecayBit and PrecisionBit** *EPJC*, [arXiv:1705.07936]
Spectrum calculation, decay widths and precision observables.
- ❸ **FlavBit** *EPJC*, [arXiv:1705.07933]
Flavour physics, observables and likelihoods.
- ❹ **ColliderBit** *EPJC*, [arXiv:1705.07919]
Collider observables and likelihoods.
- ❺ **ScannerBit** *EPJC*, [arXiv:1705.07959]
Module for scanners and printers
- ❻ **NeutrinoBit** *EPJC*, [arXiv:1908.02302]
Neutrino observables and likelihoods.
- ❼ **CosmoBit** *JCAP*, [arXiv:2009.03286]
Cosmological observables and likelihoods.



- Threshold corrections when energy scale $\mu < m_q \rightarrow$ reduced degrees of freedom:

$$\mathcal{C}_{i,q}^{(7)} = \mathcal{C}_{i,q}^{(7)} - \mathcal{C}_{i+4,q}^{(7)} \quad (i = 1, 2), \quad \mathcal{C}_{j,q}^{(7)} = \mathcal{C}_{j,q}^{(7)} + \mathcal{C}_{j+4,q}^{(7)} \quad (j = 3, 4). \quad (6)$$

- Tensor operators $\mathcal{Q}_{9,q}^{(7)}$ and $\mathcal{Q}_{10,q}^{(7)}$ mix above EW scale \implies dim-5 dipole operators:

$$\mathcal{Q}_1^{(5)} = \frac{e}{8\pi^2} (\bar{\chi} \sigma_{\mu\nu} \chi) F^{\mu\nu}, \quad \mathcal{Q}_2^{(5)} = \frac{e}{8\pi^2} (\bar{\chi} i \sigma_{\mu\nu} \gamma_5 \chi) F^{\mu\nu}. \quad (7)$$

- For $\Lambda > m_t$, $\mathcal{Q}_{9,10,t}^{(7)}$ gives a contribution to $\mathcal{Q}_{1,2}^{(5)}$ at one-loop level:

$$\mathcal{C}_{1,2}^{(5)}(m_Z) = \frac{4m_t^2}{\Lambda^2} \log\left(\frac{m_Z^2}{\Lambda^2}\right) \mathcal{C}_{9,10;t}^{(7)}(\Lambda). \quad (8)$$

- Axial-vector top-quark current $\mathcal{Q}_{3,t}^{(6)}$ mixes into operators $\mathcal{Q}_{1,q}^{(6)}$:

$$\mathcal{C}_{1,u/d}^{(6)}(m_Z) = \mathcal{C}_{1,u/d}^{(6)}(\Lambda) + \frac{2s_w^2 \mp (3 - 6s_w^2)}{8\pi^2} \frac{m_t^2}{v^2} \log\left(\frac{m_Z^2}{\Lambda^2}\right) \mathcal{C}_{3,t}^{(6)}(\Lambda).$$



ATLAS & CMS monojet searches

- Collider process: $pp \rightarrow \chi\chi j$ with missing transverse energy \cancel{E}_T .
- CMS and ATLAS monojet searches based on 36 fb^{-1} and 139 fb^{-1} of Run II data, respectively.

G. Aad et al., [arXiv:2102.10874]; A. M. Sirunyan et al., PRD, [arXiv:1712.02345]

- Expected number of events in a given bin of \cancel{E}_T distribution:

$$N = L \times \sigma \times (\epsilon A). \quad (9)$$

- Produce separate interpolations of σ and (ϵA) based on output of MadGraph_aMC@NLO, interfaced to Pythia.
- Matching between MadGraph and Pythia performed according to CKKW prescription, and detector response simulation using Delphes.
- Only $\mathcal{C}_i^{(6)}$ and $\mathcal{C}_{i=1,\dots,4}^{(7)}$ relevant for collider searches. Others suppressed by either PDFs (for heavy quarks) or mass term (for light quarks).
- Separate grids generated for operators that *do not* interfere. For $d = 6$, interference occurs between $\mathcal{Q}_{1,q}^{(6)}/\mathcal{Q}_{4,q}^{(6)}$ and $\mathcal{Q}_{2,q}^{(6)}/\mathcal{Q}_{3,q}^{(6)} \rightarrow$ parametrise tabulated grids by mixing angle θ as $\mathcal{C}_{1,2}^{(6)} = \sin \theta$ and $\mathcal{C}_{3,4}^{(6)} = \cos \theta$.



ATLAS & CMS monojet searches

- 22 and 13 exclusive signal regions in CMS and ATLAS monojet analyses, respectively.
- For CMS analysis, combine all signals using publicly available information. For ATLAS, only a single signal region used at once → maximise sensitivity by combining 3 highest \cancel{E}_T bins.
- For CMS analysis, we have

$$\mathcal{L}_{\text{CMS}}(\mathbf{s}, \boldsymbol{\gamma}) = \prod_{i=1}^{22} \left[\frac{(s_i + b_i + \gamma_i)^{n_i} e^{-(s_i + b_i + \gamma_i)}}{n_i!} \right] \frac{1}{\sqrt{\det 2\pi\Sigma}} e^{-\frac{1}{2}\boldsymbol{\gamma}^T \boldsymbol{\Sigma}^{-1} \boldsymbol{\gamma}}.$$

- Define profiled CMS likelihood ($\mathcal{L}_{\text{CMS}}(\mathbf{s}) \equiv \mathcal{L}_{\text{CMS}}(\mathbf{s}, \hat{\boldsymbol{\gamma}})$) by profiling over 22 nuisance parameters in $\boldsymbol{\gamma}$.
- For ATLAS analysis, $\mathcal{L}_{\text{ATLAS}}(s_i) \equiv \mathcal{L}_{\text{ATLAS}}(s_i, \hat{\gamma}_i)$, where i = signal region with best expected sensitivity (one with lowest likelihood when $n_i = b_i$).
- Total LHC likelihood: $\ln \mathcal{L}_{\text{LHC}} = \ln \mathcal{L}_{\text{CMS}} + \ln \mathcal{L}_{\text{ATLAS}}$.

$$\Delta \ln \mathcal{L}_{\text{LHC}} = \ln \mathcal{L}_{\text{LHC}}(\mathbf{s}) - \ln \mathcal{L}_{\text{LHC}}(\mathbf{s} = \mathbf{0}), \quad (10)$$

$$\Delta \ln \mathcal{L}_{\text{LHC}}^{\text{cap}}(\mathbf{s}) = \min [\Delta \ln \mathcal{L}_{\text{LHC}}(\mathbf{s}), \Delta \ln \mathcal{L}_{\text{LHC}}(\mathbf{s} = \mathbf{0})]. \quad (11)$$



Nuisance parameters

Nuisance parameter		Value ($\pm 3\sigma$ range)
Local DM density	ρ_0	0.2–0.8 GeV cm ⁻³
Most probable speed	v_{peak}	240 (24) km s ⁻¹
Galactic escape speed	v_{esc}	528 (75) km s ⁻¹
Running top mass ($\overline{\text{MS}}$ scheme)	$m_t(m_t)$	162.9 (6.0) GeV
Pion-nucleon sigma term	$\sigma_{\pi N}$	50 (45) MeV
Strange quark contrib. to nucleon spin	Δs	-0.035 (0.027)
Strange quark nuclear tensor charge	g_T^s	-0.027 (0.048)
Strange quark charge radius of the proton	r_s^2	-0.115 (0.105) GeV ⁻²

Table 1: List of nuisance parameters that are varied simultaneously with the DM EFT model parameters.



Type of interactions

	SI scattering	SD scattering	Annihilations
Dimension-6 operators			
$\mathcal{Q}_{1,q}^{(6)} = (\bar{\chi}\gamma_\mu\chi)(\bar{q}\gamma^\mu q)$	unsuppresssed	—	<i>s</i> -wave
$\mathcal{Q}_{2,q}^{(6)} = (\bar{\chi}\gamma_\mu\gamma_5\chi)(\bar{q}\gamma^\mu q)$	suppressed	—	<i>p</i> -wave
$\mathcal{Q}_{3,q}^{(6)} = (\bar{\chi}\gamma_\mu\chi)(\bar{q}\gamma^\mu\gamma_5 q)$	—	suppressed	<i>s</i> -wave
$\mathcal{Q}_{4,q}^{(6)} = (\bar{\chi}\gamma_\mu\gamma_5\chi)(\bar{q}\gamma^\mu\gamma_5 q)$	—	unsuppressed	<i>s</i> -wave $\propto m_q^2/m_\chi^2$
Dimension-7 operators			
$\mathcal{Q}_1^{(7)} = \frac{\alpha_s}{12\pi}(\bar{\chi}\chi)G^{a\mu\nu}G_{\mu\nu}^a$	unsuppresssed	—	<i>p</i> -wave
$\mathcal{Q}_2^{(7)} = \frac{\alpha_s}{12\pi}(\bar{\chi}i\gamma_5\chi)G^{a\mu\nu}G_{\mu\nu}^a$	suppressed	—	<i>s</i> -wave
$\mathcal{Q}_3^{(7)} = \frac{\alpha_s}{8\pi}(\bar{\chi}\chi)G^{a\mu\nu}\tilde{G}_{\mu\nu}^a$	—	suppressed	<i>p</i> -wave
$\mathcal{Q}_4^{(7)} = \frac{\alpha_s}{8\pi}(\bar{\chi}i\gamma_5\chi)G^{a\mu\nu}\tilde{G}_{\mu\nu}^a$	—	suppressed	<i>s</i> -wave
$\mathcal{Q}_{5,q}^{(7)} = m_q(\bar{\chi}\chi)(\bar{q}q)$	unsuppresssed	—	<i>p</i> -wave $\propto m_q^2/m_\chi^2$
$\mathcal{Q}_{6,q}^{(7)} = m_q(\bar{\chi}i\gamma_5\chi)(\bar{q}q)$	suppressed	—	<i>s</i> -wave $\propto m_q^2/m_\chi^2$
$\mathcal{Q}_{7,q}^{(7)} = m_q(\bar{\chi}\chi)(\bar{q}i\gamma_5 q)$	—	suppressed	<i>p</i> -wave $\propto m_q^2/m_\chi^2$
$\mathcal{Q}_{8,q}^{(7)} = m_q(\bar{\chi}i\gamma_5\chi)(\bar{q}i\gamma_5 q)$	—	suppressed	<i>s</i> -wave $\propto m_q^2/m_\chi^2$
$\mathcal{Q}_{9,q}^{(7)} = m_q(\bar{\chi}\sigma^{\mu\nu}\chi)(\bar{q}\sigma_{\mu\nu}q)$	loop-induced	unsuppressed	<i>s</i> -wave $\propto m_q^2/m_\chi^2$
$\mathcal{Q}_{10,q}^{(7)} = m_q(\bar{\chi}i\sigma^{\mu\nu}\gamma_5\chi)(\bar{q}\sigma_{\mu\nu}q)$	loop-induced	suppressed	<i>s</i> -wave $\propto m_q^2/m_\chi^2$

Table 2: Full list of dimension-6 and 7 operators included in our study, and the types of interactions they induce. Here SI (SD) = spin-independent (spin-dependent) DM-nucleon interaction.



Best-fit points

LHC likelihood	Relic density constraint	$2\Delta \ln \mathcal{L}$	Best-fit m_χ (GeV)	Best-fit Λ (GeV)	Best-fit constrained coupling combination(s) (TeV $^{-2}$)
Capped	Upper bound	0.3	5.0	< 200	$ \mathcal{C}_3^{(6)} /\Lambda^2 = 67$
Capped	Saturated	-0.5	500	> 1000	$ \mathcal{C}_2^{(6)} /\Lambda^2 = 0.22$ $ \mathcal{C}_3^{(6)} /\Lambda^2 = 0.041$
Full (hard cut-off)	Upper bound	2.2	500	> 1250	$ \mathcal{C}_3^{(6)} /\Lambda^2 = 0.14$
Full (smooth cut-off)	Upper bound	2.6	320	640	$ \mathcal{C}_3^{(6)} /\Lambda^2 = 0.18$
Full (hard cut-off)	Saturated	1.9	500	> 1250	$ \mathcal{C}_3^{(6)} /\Lambda^2 = 0.047$ $\sqrt{(\mathcal{C}_2^{(6)})^2 + (\mathcal{C}_4^{(6)})^2}/\Lambda^2 = 0.15$
Full (smooth cut-off)	Saturated	2.0	420	840	$ \mathcal{C}_3^{(6)} /\Lambda^2 = 0.052$ $\sqrt{(\mathcal{C}_2^{(6)})^2 + (\mathcal{C}_4^{(6)})^2}/\Lambda^2 = 0.23$

Table 3: Best-fit points from our various scans involving dimension-6 operators with restricted parameter ranges ($5 \text{ GeV} \leq m_\chi \leq 500 \text{ GeV}$ and $20 \text{ GeV} \leq \Lambda \leq 2 \text{ TeV}$). Here we only quote the combination that is well-constrained rather than each parameter individually.

